Available online at www.sciencedirect.com

SCIENCE DIRECT®

Marine Chemistry 95 (2005) 65–88

MARINE CHEMISTRY

www.elsevier.com/locate/marchem

Spatial and temporal distribution of Fe(II) and H_2O_2 during EisenEx, an open ocean mescoscale iron enrichment

Peter L. Croot[a,*], Patrick Laan[a], Jun Nishioka[b], Volker Strass[c], Boris Cisewski[c], Marie Boye[a], Klaas R. Timmermans[a], Richard G. Bellerby[d], Laura Goldson[e], Phil Nightingale[f], Hein J.W. de Baar[a]

[a]*Netherlands Institute for Sea Research, Postbus 59, 1790 AB Den Burg—Texel, The Netherlands*
[b]*Central Research Institute of Electric Power Industry, Japan*
[c]*Alfred Wegener Institute for Polar Research, Am Handelshafen 12, D-27570 Bremerhaven, Germany*
[d]*Bjerknes Centre for Climate Research, University of Bergen, Allègatan 55, 5007 Bergen, Norway*
[e]*School of Environmental Sciences, University of East Anglia, Norwich, United Kingdom*
[f]*Plymouth Marine Laboratory, Plymouth, UK*

Received 31 August 2003; received in revised form 7 April 2004; accepted 10 June 2004
Available online 19 February 2005

Abstract

Measurements of Fe(II) and H_2O_2 were carried out in the Atlantic sector of the Southern Ocean during EisenEx, an iron enrichment experiment. Iron was added on three separate occasions, approximately every 8 days, as a ferrous sulfate ($FeSO_4$) solution. Vertical profiles of Fe(II) showed maxima consistent with the plume of the iron infusion. While H_2O_2 profiles revealed a corresponding minima showing the effect of oxidation of Fe(II) by H_2O_2, observations showed detectable Fe(II) concentrations existed for up to 8 days after an iron infusion. H_2O_2 concentrations increased at the depth of the chlorophyll maximum when iron concentrations returned to pre-infusion concentrations (<80 pM) possibly due to biological production related to iron reductase activity.

In this work, Fe(II) and dissolved iron were used as tracers themselves for subsequent iron infusions when no further SF_6 was added. EisenEx was subject to periods of weak and strong mixing. Slow mixing after the second infusion allowed significant concentrations of Fe(II) and Fe to exist for several days. During this time, dissolved and total iron in the infusion plume behaved almost conservatively as it was trapped between a relict mixed layer and a new rain-induced mixed layer. Using dissolved iron, a value for the vertical diffusion coefficient K_z=6.7±0.7 $cm^2\ s^{-1}$ was obtained for this 2-day period. During a subsequent surface survey of the iron-enriched patch, elevated levels of Fe(II) were found in surface waters presumably from Fe(II) dissolved in the rainwater that was falling at this time.

Model results suggest that the reaction between uncomplexed Fe(III) and O_2^- was a significant source of Fe(II) during EisenEx and helped to maintain high levels of Fe(II) in the water column. This phenomenon may occur in iron enrichment

* Corresponding author. Now at FB2: Marine Biogeochemie, Leibniz Institut für Meereswissenschaften (IFM-GEOMAR) und CAU Kiel, Düsternbrooker Weg 20, 24105 Kiel, Germany.
E-mail address: pcroot@ifm-geomar.de (P.L. Croot).

0304-4203/$ - see front matter
doi:10.1016/j.marchem.2004.06.041

experiments when two conditions are met: (i) When Fe is added to a system already saturated with regard to organic complexation and (ii) when mixing processes are slow, thereby reducing the dispersion of iron into under-saturated waters.

Keywords: Fe(II) and H_2O_2; Iron enrichment experiment; EisenEx

1. Introduction

The question of what role does iron play in controlling phytoplankton biomass and productivity in the High Nutrient Low Chlorophyll (HNLC) regions of the global ocean (de Baar and Boyd, 1999; Martin et al., 1989, 1990) now appears to be answered. The first mesoscale iron enrichments in the Equatorial Pacific, IRONEX I and II (Coale et al., 1996; Martin et al., 1994), and in the Southern Ocean, SOIREE, (Boyd and Law, 2001), have answered in the affirmative by dramatic demonstration of intense phytoplankton growth after relief of iron limitation. However, there is still much to be learnt from iron enrichment experiments, notably insight into mechanisms of biogeochemical cycling of iron and other nutrients. This paper describes results from EisenEx (Smetacek, 2001), a mesoscale iron enrichment experiment in the Atlantic sector of the Southern Ocean performed in October/November 2000. Further mesoscale experiments have taken place since EisenEx in the Southern Ocean, SOFeX, and in the North Pacific, SEEDS (Tsuda et al., 2003) and SERIES.

All of the open ocean mesoscale iron enrichment experiments performed to date have used ferrous sulfate ($FeSO_4$) as their iron source for the additions. This Fe^{II} source is significantly more soluble than Fe^{III}, the thermodynamically favoured form; however, Fe^{II} is rapidly oxidised to Fe^{III} by O_2 and H_2O_2 in warm waters(Millero and Sotolongo, 1989; Millero et al., 1987). Fe^{III} rapidly forms complexes with hydroxide with subsequent formation of colloidal oxyhydroxide (Kuma et al., 1996) species which lately coagulate and form particulate iron (Johnson et al., 1997). The overall process causes a loss of dissolved iron (half-life 10–30 h; Gordon et al., 1998), as seen in early mesoscale iron enrichments performed in the Equatorial Pacific IronEX I (Gordon et al., 1998), IronEX II (Coale et al., 1996) and the Southern Ocean (Bowie et al., 2001). In the cold waters of the Southern Ocean, the oxidation rate for Fe^{II} is significantly slower (Croot et al., 2001) and Fe^{II} can became a significant proportion of the iron species in seawater. The present work examines the spatial and temporal changes in Fe^{II} and H_2O_2, a key oxidant of Fe^{II}, during the EisenEx experiment.

1.1. Iron speciation in seawater

The overall speciation of Fe^{III} in seawater has been found to be dominated by complexation with organic ligands (Boye et al., 2001; Croot and Johansson, 2000; Rue and Bruland, 1995; van den Berg, 1995), believed to be produced by bacteria or phytoplankton. The inorganic speciation of Fe^{III} is strongly influenced by $Fe(OH)_x$ species (Byrne et al., 1988; Millero et al., 1995; Turner et al., 1981). The solubility of Fe^{III} in seawater has recently been investigated over a range of ambient temperatures by Liu and Millero (2002). These authors found that in the absence of organic ligands the iron solubility is controlled by the solubility of the dominant $Fe(OH)_x$ species, with an increase in solubility with decreasing temperature, though presently there are no measurements below 5 °C. The presence of iron complexing ligands increases the overall solubility of iron in seawater (Öztürk et al., 2004).

The equilibrium inorganic speciation of Fe^{II} in ambient seawater at 25 °C is strongly influenced by the ferrous carbonate complex, $Fe(CO_3)$ (King, 1998). Organic complexation of Fe^{II} in seawater is suspected (Croot et al., 2001), based on slower Fe^{II} oxidation rates, but as yet no definitive evidence has been presented. Fe(II) has been shown to be formed from photochemical processes in seawater, noticeably in the presence of uronic acids (Kuma et al., 1992; Öztürk et al., 2004). Presently, there is also little information on the effect of temperature on Fe^{II} speciation, as most studies have been undertaken at 25 °C.

1.2. Redox cycling of iron in seawater

In recent years, there have been a number of important contributions towards understanding the redox cycling of iron in seawaters. The mechanism proposed for the oxidation of Fe^{II} in seawater by King et al. (1995) has been widely accepted for studies of iron speciation and redox cycling in natural systems (Emmenegger et al., 1998; King, 1998; King and Farlow, 2000; Rose and Waite, 2002; Voelker et al., 1997).

$$Fe(II) + O_2 \xrightarrow{k_1} Fe(III) + O_2^- \quad (1)$$

$$2H^+ + Fe(II) + O_2^- \xrightarrow{k_2} Fe(III) + H_2O_2 \quad (2)$$

$$Fe(II) + H_2O_2 \xrightarrow{k_3} Fe(III) + OH^- + HO^\bullet \quad (3a)$$

$$Fe(II) + H_2O_2 \xrightarrow{k_3} Fe(IV)O^{2+} + H_2O \quad (3b)$$

$$Fe(II) + HO^\bullet \xrightarrow{k_4} Fe(III) + OH^- \quad (4)$$

The reaction between Fe(II) and H_2O_2 (Eq. (3a), usually called the Fenton reaction) was originally proposed to form the hydroxyl radical, but recent reviews present more evidence for the formation (Eq. (3b)) of the ferryl ion $Fe(IV)O^{2+}$ (Dunford, 2002; Kremer, 1999; Pierre and Fontecave, 1999). The ferryl ion subsequently reacts with either H_2O_2 to reform Fe^{II} and O_2, or alternatively with Fe^{II} to produce Fe^{III}. In many cases, the reactivity of the ferryl ion and the hydroxyl radical with organic substrates are indistinguishable, making elucidation of which mechanistic pathway occurs difficult.

For reaction (4), it has been shown that in natural waters the hydroxyl radical probably reacts with other ions (e.g. Br^-, Cl^- and CO_3^{2-}), but subsequently the newly produced radicals can also oxidize Fe^{II} (King et al., 1995); however, at low Fe^{II} concentrations, reactions between the hydroxyl radical and dissolved organic matter (DOM) will predominate (Emmenegger et al., 1998).

There is also the possibility of a back reaction between Fe^{III} and superoxide (King et al., 1995; Voelker and Sedlak, 1995).

$$Fe(III) + O_2^- \xrightarrow{k_5} Fe(II) + O_2 \quad (5)$$

Voelker and Sedlak (1995) estimated that in the absence of organic complexation of Fe^{III}, 30–75% of the dissolved iron would be present at Fe^{II} during daytime. Organic iron complexes appear to be much less reactive with O_2^-. Subsequent work has suggested that similar reactions with inorganic Cu are an important sink of O_2^- in seawater (Zafiriou et al., 1998). Organic complexation of Fe^{II} in laboratory experiments has shown that ligands that form strong Fe^{III} complexes promote/increase the oxidation rate, while some ligands can completely inhibit the oxidation (Santana-Casiano et al., 2000; Theis and Singer, 1974).

1.3. Hydrogen peroxide

Hydrogen peroxide (H_2O_2) is the most stable intermediate in the four-electron reduction of O_2 to H_2O and may function as an oxidant or a reductant (see above). H_2O_2 is principally produced in the water column by photochemical reactions involving DOM and O_2 (Cooper et al., 1988; Scully et al., 1996; Yocis et al., 2000; Yuan and Shiller, 2001). DOM and O_2 react to produce the short-lived radical species superoxide (O_2^-), which undergoes disproportionation to form H_2O_2.

$$2O_2^- + 2H^+ \rightarrow H_2O_2 \quad (6)$$

In the open ocean, H_2O_2 concentrations show a distinct exponential profile with a maximum at the surface consistent with the photochemical flux. Concentrations can reach up to 300 nmol L^{-1} in equatorial and tropical regions with high DOM concentrations such as in the Amazon plume in the Atlantic (Yuan and Shiller, 2001). In regions with low DOM and low sunlight, surface H_2O_2 levels are much lower with typical values in the Antarctic of 10–20 nmol L^{-1} (Resing et al., 1993; Sarthou et al., 1997).

H_2O_2 can also be produced by biological processes in the ocean, such as glycolate oxidation during photorespiration (Lehninger, 1979), and dark produc-

tion has been observed in the Sargasso Sea (Palenik and Morel, 1988) and in phytoplankton cultures (Palenik et al., 1987). Most phytoplankton possess the enzyme superoxide dismutase (SOD) which catalyses the conversion of superoxide to H_2O_2, and this may be one of many biological reactions producing H_2O_2 in seawater. However, most studies to date have shown that the major production pathway in the water column is from photochemical production, in a few cases, notably the Southern Ocean, distinct H_2O_2 maximums at depth (Sarthou et al., 1997), corresponding to the chlorophyll maximum, suggest a significant biological source of H_2O_2.

H_2O_2 can react in the water column with a number of other chemical species via a variety of pathways. Reactions with metal species such as Fe(II), via reactions (3a) and (3b), and Cu(I) can lead to the destruction of H_2O_2 The decay of H_2O_2 appears to obey first-order kinetics (Petasne and Zika, 1997; Yuan and Shiller, 2001) and is biologically mediated by small microorganisms (Petasne and Zika, 1997). This 'dark decay lifetime' of H_2O_2 can vary from hours to weeks in the ocean (Petasne and Zika, 1997), but typically may be around 4 days in the open ocean (Plane et al., 1987). Filtration of seawater to remove the biota typically results in a dramatic reduction in the decay rate of H_2O_2 (Moffett and Zafiriou, 1990; Petasne and Zika, 1997). Isotopic studies of the decomposition of H_2O_2 have found that 65–80% of the decay was from catalase activity (reduction to H_2O and O_2) with 20–35% from peroxidase activity (reduction to H_2O only) (Moffett and Zafiriou, 1990). The amount of colloidal material has also been shown to influence the decay rate of H_2O_2 (Yuan and Shiller, 2001). Overall, the decay rate of H_2O_2 is apparently controlled by several factors: H_2O_2 concentration, colloid concentration, bacteria numbers and temperature (Yuan and Shiller, 2001).

The same photochemical processes that form H_2O_2 in seawater also take place in atmospheric waters, leading to high concentrations of H_2O_2 in atmospheric water which can reach the sea surface as rain. Rainwater concentrations of H_2O_2 can vary from 2 to 60 μmol L^{-1} (Kieber et al., 2001a,c; Yuan and Shiller, 2000) depending on the meteorological conditions prior to precipitation. Rainwater can be a considerable source of H_2O_2 to the surface mixed layer.

Other papers in this volume examine other aspects of the iron cycling in EisenEx, including; the fate of the added iron (Croot et al., submitted for publication), changes in the size fractionation of iron (Nishioka et al., 2004) and in organic iron complexation (Boye et al., submitted for publication). A further paper also report results of deckboard experiments designed to examine the effect of natural UV irradiation on the photoreduction of iron (Rijkenberg et al., in press).

2. Methods

2.1. Sampling

Samples were collected during cruise ANT XVIII/2 (Oct.–Nov. 2000) on the German research vessel *P.S. Polarstern* during the mesoscale iron enrichment experiment EisenEx (Smetacek, 2001). During this experiment, three iron infusions, on 8-day intervals, were performed in an SF_6-labelled patch in a mesoscale eddy (diameter ~100–150 km) that had originated from the southern Polar Front (Fig. 1) and subsequently drifted 400 km north to the experimental site. The iron was added as an acidic ferrous sulfate solution in seawater and released at approximately 30 m below the surface by means of a towed drogue. Further details on the method of iron infusions can be found in Croot et al. (submitted for publication). A timeline of major sampling events and infusions is found in Table 1.

Vertical sampling and underway surface measurements were performed inside and outside the SF_6-labelled patch and the 'in stations' were situated at the position of the highest observed SF_6 concentrations, whereas 'out stations' were located in waters of the eddy which displayed background SF_6 concentrations (Watson et al., 2001). The timing of the iron infusions and of significant large-scale underway mapping exercises for Fe(II) are shown in Table 1.

Underway temperature, nutrients and chlorophyll *a* data of the surface were derived from Polarstern's pumping system located at the bow of the ship at 8 m depth. Conductivity–temperature–depth (CTD) profiles were obtained using a Sea-Bird Electronics SBE 911plus on a 24-bottle rosette (Sea-Bird SBE32, not used for trace metal sampling). Meteorological data, wind speed and direction, precipitation, humidity, air temperature, and photosynthetically available radia-

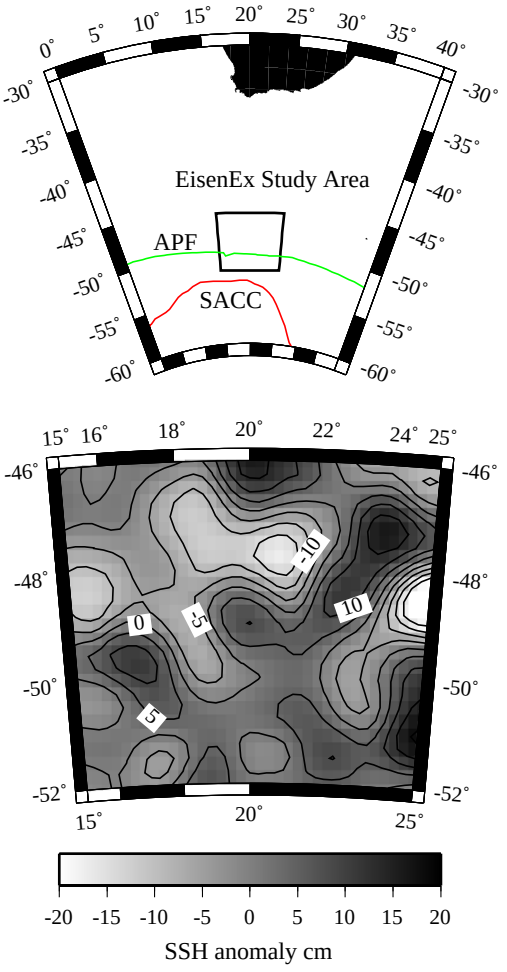

Fig. 1. Top: The Atlantic sector of the Southern Ocean, showing the EisenEx study area. The approximate positions of the Antarctic Polar Front (APF) and the Southern Antarctic Circumpolar Current (SACC) are also shown. The EisenEx eddy was originally from waters south of the APF. Bottom: Satellite-derived sea surface height anomaly over the study region for November 2000—the EisenEx eddy is visible as a depression at approximately 21°E, 48°S. The sea surface height anomaly data was kindly provided by the Colorado Center for Astrodynamics Research, University of Colorado, Boulder, and was derived from TOPEX/POSEIDON data using a climatological mean acquired during the period 1993–1996.

tion (PAR), were obtained from onboard instrumentation on the Polarstern. Wind stress was calculated according to Price et al. (1986):

$$\tau = \rho_a C_D U^2$$

where ρ_a=1.23 kg m^{-3} is the density of air, U is the true wind speed (m s^{-1}) and C_D (1.3–1.6×10^{-3}) is the drag coefficient computed by the Large and Pond (1981) formulation. Meteorological data was collected on 1-min intervals and the data reported in this paper is constructed from 10-min averages of the raw data. All data in this work is reported according to the decimal day 2000 time frame (Table 1).

Analytical trace work was carried out in an over-pressurized class 100 clean air van (de Jong et al., 1998), inside of which analysts wore special antistatic lab coats and caps, clogs and plastic gloves. The van is equipped with an Elgastat reverse osmosis filter and water purification equipment delivering >18 MΩ deionised water (DI).

2.2. Sampling of surface seawater

Surface sampling was done by pumping seawater into the clean air container through a tube attached to a towed fish. Contamination from the ship was avoided by towing the fish at ~5 m distance alongside the ship with the crane arm of a hydrographic winch, keeping it outside the ships wake. The fish was a homemade, 1-m-long solid stainless steel, epoxy-coated torpedo of 50 kg with three fins at the tail. The fish remained stable at a depth of 2–3 m at speeds up to the maximum cruising speed of 14.7 knots. The sample tubing consisted of ~15 m flexible reinforced

Table 1
Timeline of Fe(II) surface sampling transect information for EisenEx

Transect no.	Date (DD)	Time (UTC)	
First release	Nov. 7 Nov. 8	17:20–06:45	Release of Fe and SF_6
3	Nov. 8 (313)	12:30–18:23	
4	Nov. 9 (314)	02:10–08:51	
5	Nov. 14 (319)	09.47–13:15	
6	Nov. 15 (320)	16:09–18:54	
Second release	Nov. 15 Nov. 16	22:30–12:30	Only Fe release
7	Nov. 17 (322)	07:20–09:19	
8	Nov. 18 (323)	No sampling	
9	Nov. 19 (324)	08:56–10:27	
Third release	Nov. 24 (329)	07:45–19:15	Only Fe release
10	Nov. 25 (330)	06:20–08:43	
11	Nov. 25–26 (330–331)	19:00–17:17	

DD denotes decimal day, where 12:00 UTC on the 1st January is defined as 1.5000.

PVC, 10 mm i.d. It was attached with tape and tie-wraps to the fish and the stainless steel hydrowire. The tubing had been extensively cleaned with 1M HCl and rinsed with DI water. The water was pumped onboard with an Almatec A-15 Teflon diaphragm pump. The seawater was filtered in-line at a flow rate of 2–3 L min^{-1} through a Sartorious Sartobran filter cartridge (0.4 μm prefilter and 0.2 μm final filter). Discrete samples for dissolved iron were taken in 100 mL clean polyethylene bottles (Kartell) and acidified to pH 1.8 with triple quartz distilled (3QD) concentrated hydrochloric acid (1 mL L^{-1}). All sample bottles had been cleaned by leaching in hot (60 °C) 6 M HCl for at least 24 h followed by ample rinsing with DI water.

For continuous Fe(II) sampling, a secondary Teflon line downstream of the filter was connected directly to the Fe(II) analysis system and the sample drawn through the ante room into the clean room using a Gilson minipulse peristaltic pump. The lag time between sample collection, at the head of the towed fish, to arrival at the detector was estimated to be approximately 120 s (Croot and Laan, 2002).

2.3. Sampling of near surface waters

For vertical sampling of seawater, modified Teflon-coated PVC General Oceanics (Miami, FL, USA) GO-FLO bottles of 11 L were used. The original drain cock had been replaced by a Teflon stopcock. The cleaning procedures and handling of the GO-FLO bottles has been described early (de Jong et al., 1998). Immediately upon recovery of the bottles, samples were filtered in-line through 0.2 μm filter cartridges (Sartorious Sartobran filter capsule 5231307H5) by N_2 overpressure into acid-cleaned sampled bottles: 60 mL Teflon bottles (Nalgene) for Fe(II) analysis immediately, 100 mL polyethylene bottles (Kartell) for dissolved and total iron (unfiltered samples) analysis. Nutrient samples were also drawn from each GO-FLO bottle and analysed onboard using a Technicon II Autoanalyzer following standard methods. The temperature and pressure at which the GO-FLO bottles closed were recorded by SIS (Sensoren Instrumente Systeme GmbH) electronic reversing instruments, the RTM 4002 X and RPM 6000 X, respectively, which had previously been calibrated in the laboratory at NIOZ.

2.4. Dissolved and total iron

Dissolved iron (DFe—defined here as that Fe which passed through a 0.2-μm filter cartridge) and total iron (TFe—unfiltered) was determined as Fe(III) using a chemiluminescence flow injection method employing luminol and H_2O_2 (de Jong et al., 1998). Typical detection limits and blank values for this system at the time of operation were 0.021 and 0.022 nM, respectively.

2.5. Fe(II) analysis

For the determination of Fe(II), a highly sensitive chemiluminescence flow injection analysis system was used and full details can be found in Croot and Laan (2002). In brief, this technique uses the reaction between Fe(II) and O_2 to produce O_2^-, which rapidly reacts with a luminol radical to an electronically excited aminophtalate and N_2 (Rose and Waite, 2001; Xiao et al., 2002). Light is emitted as the aminophtalate returns to the ground state and this is the basis of the chemiluminescence technique; more details can be found in Rose and Waite (2001). For the present work, no preconcentration of Fe(II) was performed so as to eliminate possible artifacts from pH or redox environment changes imposed by the preconcentration step. Previous work with Fe(II) and ferroin-based ligands has shown that column-based methods can easily overestimate in situ Fe(II) concentrations (Croot and Hunter, 2000).

Samples from vertical profiles were maintained at the ambient seawater temperature (3–4 °C) to maintain oxidation of Fe(II) at in situ rates. The maximum time between sample collection, GO-FLO bottle closing, and analysis was 20 min. The detection limit for this technique during this work (all analysis) ranged from 4 to 250 pM, and depended mostly on the background chemiluminescence from the luminol reagent. In general, lower detection limits were found for the vertical sampling where replicates could be run, than for the continuous underway sampling. Only the data that was at least three standard deviations of the blank above the detection limit are reported here for the continuous underway sampling.

2.6. Determination of H_2O_2

The concentration of H_2O_2 was determined using a fluorescent technique involving the enzyme catalysed dimerization of (*p*-hydroxy-phenyl)acetic acid (POH-PAA) (Miller and Kester, 1988). This method measures the total peroxide in seawater; this includes organic peroxides as well as H_2O_2, the concentration of the organic peroxide can be determined separately by prior removal of the H_2O_2 by the use of catalase. H_2O_2 standards were calibrated by titration with standardised KI.

2.7. Underway pH

During this cruise, the surface seawater pH was measured using the automated marine pH sensor (AMpS) system as described in Bellerby et al. (2002). This system is an automated spectrophotometric pH sensor that makes dual measurements of sulfonephthalein indicator in a semi-continuous seawater stream. The pH data used in this study were computed using the 'total hydrogen ion concentration scale'. The Fe(II) oxidation rate data of Millero and Sotolongo (1989) and Millero et al. (1987) were corrected from the free pH scale (Tris buffers in seawater) used in that work, to the total hydrogen ion concentration scale using the appropriate algorithms (DOE, 1994).

2.8. SF_6 measurements

Underway SF_6 measurements was achieved by an automated sparge-cryogenic trap system coupled to an Electron Capture Detector-Gas Chromatograph (ECD-GC), as previously described in Law et al. (1998). Surface water was obtained from the ships nontoxic surface supply and analysed in continuous mode, with a measurement obtained every 3.5 min. Underway SF_6 data is reported here as an SF_6 anomaly from that expected from equilibrium with the atmosphere (2 fmol L^{-1}), thus when there is no added SF_6, i.e. an 'out station', the underway surface SF_6 is reported as 0. Vertical profiles of SF_6 were performed on 350 mL water samples obtained from CTD hydrocasts using a discrete vacuum-sparge cryogenic trap system (Law et al., 1994).

2.9. 1D modelling of Fe(II) and H_2O_2 distribution

A simple one-dimensional chemical mixing model was constructed to examine the temporal changes in the vertical distribution of Fe(II) and H_2O_2 after the initial iron infusions. The model was solved numerically by a fully explicit finite differencing procedure over a 100-m water column. A no flux boundary condition was imposed at the surface and the depth of the mixed layer was fixed (60 m). Mixing was proscribed by the use of a vertical diffusion coefficient, with different values for above and below the mixed layer. The model was written in C and run on a PC under Windows XP, each model run simulated 24 h and took 1–10 min to run using a notebook with a 1 GHz Intel Pentium 4 processor (see below). Two versions of the model were run for this paper: (1) Chemical model incorporating only reactions (1) and (3a) (3b with reactions (2) and (4) assumed to happen instantaneously (implies a 2:1 ratio of Fe(II) to reactions with O_2 and H_2O_2). This version has no O_2^-. (2) Chemical model incorporating reactions (1–3b) and (5), thus allowing the back reaction of Fe(III) with O_2^-. There was no organic complexation of iron in the model runs presented here.

As the reaction rates with O_2^- are very rapid (see Table 2), a time step of 0.1 s was used to ensure stability of the equations, when O_2^- was not

Table 2
Reaction rate data for oxidation of Fe(II) in seawater

	Rate constant ($L\ mol^{-1}\ s^{-1}$)[a]	Source	Temperature dependence
Reaction			
O_2+Fe(II)	0.5028	Millero et al., 1987	Yes
$O_2^{\bullet-}$+Fe(II)	1×10^7	Rush and Bielski, 1985	No
	7.2×10^8	Matthews, 1983	
H_2O_2+Fe(II)	17,545	Millero and Sotolongo, 1989	Yes
$OH^{\bullet}$+Fe(II)	3×10^8	Rush and Bielski, 1985	No
Other reactions			
$O_2^{\bullet-}$+Fe(III)	5×10^7	Rush and Bielski, 1985	No
	1.8×10^8	Matthews, 1983	

[a] Calculated for pH 8.000, 4.2 °C, 35 S.

included a time step of 1 s could be used. Initial conditions were assumed that were typical for the conditions found in EisenEx. The calculated values of H_2O_2, O_2^-, Fe(II) and Fe(III) were saved to a file every 300 s of model time, the resulting output file was further processed in MATLAB™. A full version of this model based on the Price–Weller–Pinkel model (Price et al., 1986), including the effects of iron solubility, organic complexation and sunlight, is currently being developed and written up for publication.

3. Results and discussion

3.1. Effect of iron on biota

The addition of iron in EisenEx saw four- to sixfold increases in chlorophyll *a* and in primary productivity inside the patch relative to outside the patch (Gervais et al., 2002). First changes were seen in the photosynthetic efficiency of the phytoplankton (F_v/F_m) with increases from 0.3 initially inside and outside the patch to 0.55 inside the patch (Gervais et al., 2002). Nano- and microphytoplankton biomass increased but picophytoplankton biomass hardly changed (Gervais et al., 2002).

3.2. Hydrography during the EisenEx

During the course of the experiment (Nov. 6–29, 2000—decimal days 311 to 334), surface water temperatures increased from 3.5 to 4.2 °C (Gervais et al., 2002). This warming was probably mostly from increasing solar irradiation during the austral summer, though the phytoplankton bloom itself may have contributed by trapping heat in the mixed layer. Similarly, the bloom affected the vertical attenuation coefficient for downwelling irradiance which was between 0.070 and 0.083 m^{-1} (67–55 m euphotic depth) outside the patch but steadily increased to 0.114 m^{-1} (41 m euphotic depth) inside the patch (Gervais et al., 2002). Mixed layer depth (z_{ml}) was highly variable throughout the course of the experiment and was typically less than 40 m during the first 2 weeks but increasing to greater than 80 m over the last 2 weeks of the experiment (Gervais et al., 2002). The initially shallow mixed layers over the first 2 weeks were caused by wind speeds distinctly lower than the seasonal average (Dentler, 2001), a return to a more typical situation for the ACC (Mitchell et al., 1991) occurred in the third week when wind speeds peaked at over 20 m s^{-1}.

The cyclonic eddy used in this experiment was selected on the basis of sea surface height anomaly data (Fig. 1) and in situ Acoustic Doppler Current Profiler (ADCP) mapping of the flow field. The eddy was centered at 47°50′S and 20°45′E, was approximately 120 km wide and occupied an area of about 11,000 km^2. Drift buoys deployed in the patch followed a closed eddy circulation with superimposed tidal and inertial motions, they also revealed, along with ADCP data, that the eddy centre shifted slightly southerly to 48°12′S by Nov. 20, and then returned to the north (Strass et al., 2001). The general motion of patch was as expected a clockwise circulation, further wind and inertial motions and current shear influenced the overall shape of the patch.

Linear regression of the estimated patch area versus time suggests (Okubo, 1971) a horizontal diffusivity of 90 ± 30 m^2 s^{-1}. This value is one to two orders of magnitude higher than that found in previous open ocean SF_6 release experiments, including SOIREE 4 ± 2 m^2 s^{-1} (Abraham et al., 2000) and IronEX I 25 ± 5 m^2 s^{-1} (Stanton et al., 1998). It should be noted however both horizontal and vertical mixing during EisenEx was not uniform throughout the experiment. Wind-induced mixing was greatest during the passage of two major storm systems while current-induced shear mixing was a function of the velocity field of the eddy. Highest ADCP near surface currents, 40–50 cm s^{-1}, were found in the northeastern part of the eddy, close to the vicinity of the first infusion, while the slowest currents were in the southern part of the eddy, ~10 cm s^{-1} near the site of the second infusion (Strass et al., 2001).

3.3. Fe(II) initial distribution

The initial release of Fe(II) is rapidly diluted into the ship's wake and this almost instantaneous mixing forms the initial conditions for subsequent reactions involving Fe(II). Thus in order to understand the subsequent reactions and lifetime, it is important and necessary to estimate the expected concentration of

Fe(II) immediately upon injection. An earlier study by Coale et al. (1998) for Iron-Ex I applied the tracer dilution experiments of Csanady (1978) to this problem. Using this approach (see Csanady, 1978 for full details), we estimate an initial Fe(II) concentration of 72.5 nM for EisenEx (Ship's draft 8 m, beam 25 m, flow rate 2000 L h^{-1}, Fe(II) in outflow = 464 mol m^{-3}, average speed 8 km h^{-1}). This is less than the 162 nM estimated for IronEX-I (Coale et al., 1998) and 156 nM estimated for SOIREE (P. Croot, unpublished data). However, examination of initial CTD profiles after the first iron infusion revealed significant anomalies in the transmission data (Fig. 2). These anomalies were consistent with the iron plume, as they were found only for stations inside the patch, as identified by the presence of high concentrations of SF_6. Estimation of the dispersion from these transmission anomalies, apparently caused by the absorbance of light by high concentrations of colloidal or particulate iron, can give an indication of the initial mixing plume. Calculation of the dispersion was made using second moments (Law et al., 2001), from the relevant transmission data, using the apparent transmission anomaly:

$$\mathrm{Tr}_{\mathrm{an},z} = \mathrm{Tr}_z - \mathrm{Tr}_{\mathrm{mean}}$$

where $\mathrm{Tr}_{\mathrm{an},z}$ is the transmission anomaly, Tr_z is the transmission value at depth z and $\mathrm{Tr}_{\mathrm{mean}}$ is the mean transmission for the mixed layer above the transmission anomaly. Calculation of the second moment is then carried out using the following equation:

$$M2 = \frac{\int C(z - z_0)^2 \partial z}{\int C \partial z}$$

where C is the transmission anomaly (or concentrations of any other species), z_0 is the depth of the maximum in the anomaly, and z is the depth below the surface. Second moments calculated this way varied from 16 to 20 m^2. Calculation of the dilution volume using the transmission anomaly approach yielded an initial concentration of Fe(II) of 369 nM, assuming the plume is radially distributed with a radius of 8–10 m—as evidenced by the transmission anomalies in the vertical. This approach yields a significantly higher Fe(II) concentration than the estimate from the Csanady method. In the present case, the iron was released at 30–40 m depth, considerably deeper than in the work of Csanady (typically 1–2 m) and indeed was probably below the mixing zone of the Polarstern's wake

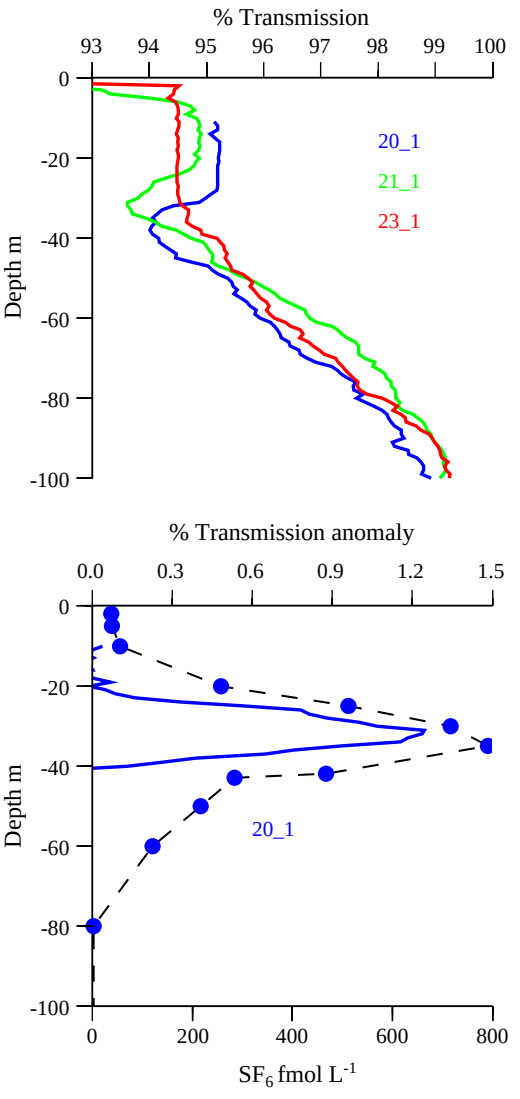

Fig. 2. (a) Transmission data from CTD profiles at stations after first iron infusion, showing the influence of the iron plume on the transmission at 30–40 m depth. Station 23_1 was located outside the SF_6 patch, while Stations 20_1 and 21_1 were inside the patch. (b) Calculated transmission anomaly (solid line) and SF_6 (circles and dotted line) concentrations for Station 20_1 (see text for details).

leading to a reduction of the initial dispersion of the patch. This was indeed intentional so as to minimize SF_6 losses to the atmosphere via bubble formation in the wake.

Total iron concentrations measured at Station 20 (Croot et al., submitted for publication) showed a distinct maximum at 40 m depth, the centre of the transmission anomaly and the added SF_6 (Fig. 2b), of 23.7 nM; however, it is not clear whether the total iron measurement includes all the Fe(II) that was probably present (see below). Unfortunately, no vertical Fe(II) or H_2O_2 measurements were made during the period between the first and second iron infusions.

For the subsequent infusions, application of the transmission anomaly approach at later time points during EisenEx is not possible because of the effect of the increased biomass scattering/absorption of light in the mixed layer. Indeed, after the second iron infusion, there is no similar transmission anomaly apparent because of the increased biomass since the first infusion. As there was no addition of SF_6 apart from the first infusion, the remaining SF_6 has limited use as a vertical tracer in the mixed layer as only processes which deepen the mixed layer will change the SF_6 vertical distribution.

3.4. Fe(II) vertical distribution

Samples for vertical profiles of Fe(II) were taken routinely after the second infusion, Fe(II) concentrations and station information along with dissolved iron concentrations from the same bottles can be found in Appendix A. In general, Fe(II) was only found at significant levels above the limit of detection at stations in the core of the patch within 2–3 days after an iron infusion. The initial distribution of Fe(II) after the second infusion (Fig. 3—Station 46) showed a maximal concentration of 1 nM at 30 m depth, consistent with the recent release of Fe(II) at that depth. Only a small amount of Fe(II) had reached 40 m depth at this time, indicating slow mixing of the iron infusion to the bottom of the mixed layer (65 m at this time). Dissolved iron (Appendix A) showed a similar trend to Fe(II), though with elevated concentrations indicating that much of the Fe(II) had been oxidized during the time (1.5–15.5 h) since the infusion began. Almost 2 days later (Station 49), however, the Fe(II) plume was still discernable in the water column although it was reduced and had dispersed over a wider depth range. A further 2 days later (Station 61), Fe(II) concentrations were further reduced and by 7 days (Station 83) there was no detectable Fe(II) remaining.

Analysis of the longevity of the Fe(II) from the infusion is complicated however by the one time use of SF_6 in this study. This is because the subsequent iron additions could not be adequately tracked using SF_6 as the supplemental iron infusions were only in a subset of the SF_6-labelled patch. Thus an 'IN' patch determination by SF_6 did not necessarily contain any of the additional infusions of iron, though it of course still had residual iron from the first infusion, this situation increased with each infusion, when the 50 km^2 infusion was carried out in a ~500 (DD320) or 800 (DD328) km^2 patch. An example of this phenomenon was after the third infusion, when the newly infused iron patch was not sampled until 3 days after its creation, by which time it was well mixed (Fig. 4) in after the passage of two storm fronts.

3.5. Mixing of iron after the second infusion

The apparently slow mixing of Fe(II) after the second iron infusion was investigated further as an attempt to try and understand the processes affecting iron cycling at this time. Normally, second moment calculations for iron or Fe(II) have the inherent problem that Fe(II) is also lost by oxidation and Fe(III) by precipitation and coagulation of particles which sink from the mixed layer. Thus the usual non-conservative behavior of iron does not allow the use of second moments to estimate mixing. However, using data from Stations 46 and 49, it is apparent, within the scope of the limited data sets, that the inventories for dissolved and total iron (Croot et al., submitted for publication) are remarkably consistent: TFe: 198 ± 15 and 227 ± 15 μmol m^{-2}; DFe: 97 ± 8 and 114 ± 8 μmol m^{-2} (Station 46 numbers reported first, integration from 20 to 100 m). There was seemingly little dilution of the Fe by horizontal dispersion at this time as the width of the surface Fe(II) patch on DD322, surface transect 7 performed in between Stations 46 and 49, was remarkably similar to the original width of the

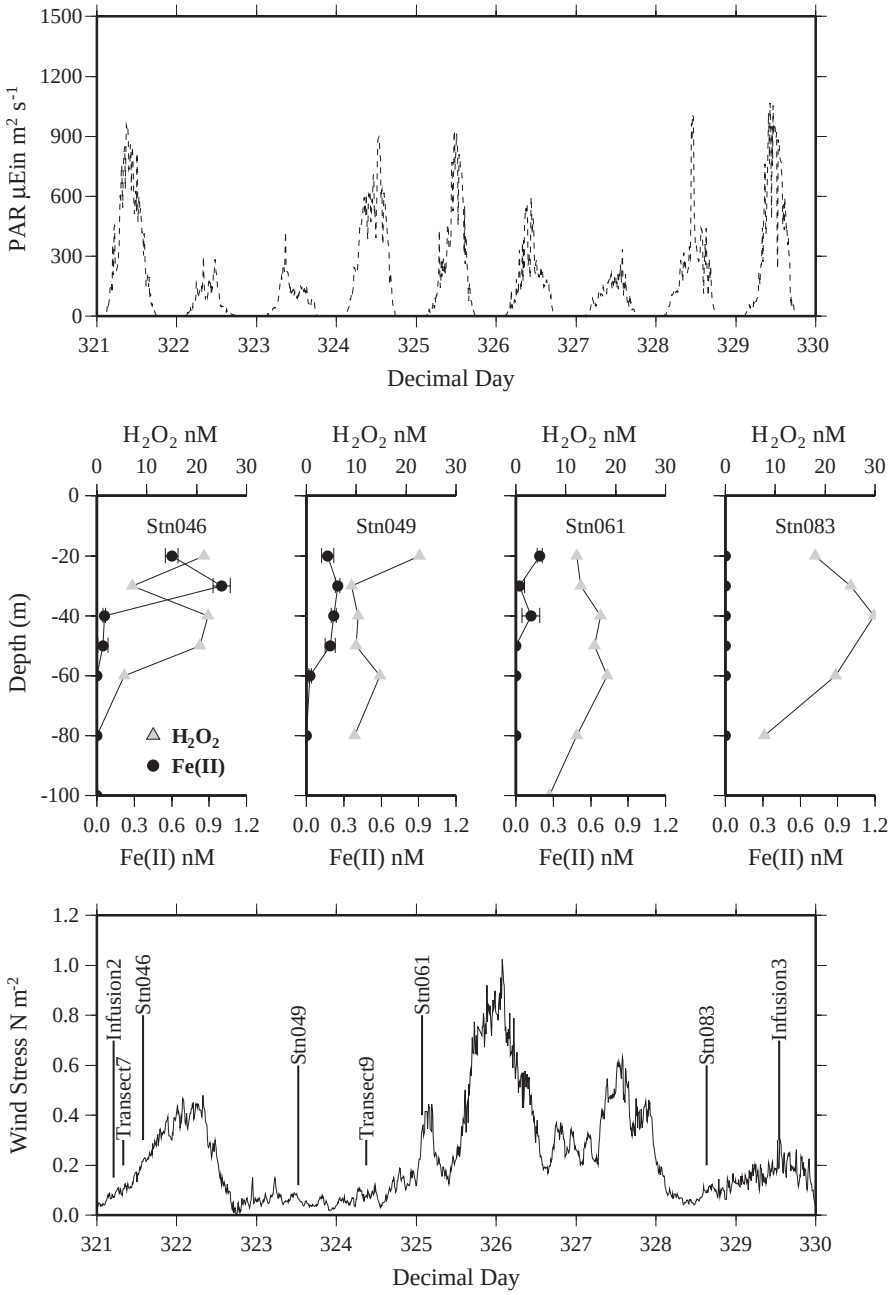

Fig. 3. Time course of vertical distribution of Fe(II) and H_2O_2 during the period between the second and third iron infusions during EisenEx. Top: Photosynthetically available radiation (PAR: 400–700 nm). Centre: H_2O_2 (triangles) and Fe(II) (circles) vertical distributions. Bottom: Wind stress and station timeline.

second infusion. The low current shear in the region of the second infusion may also imply low horizontal dispersion at this time (Strass et al., 2001). Thus estimates for the vertical diffusivity in the vicinity of the iron infusion could be obtained by using the second moment method (Law et al.,

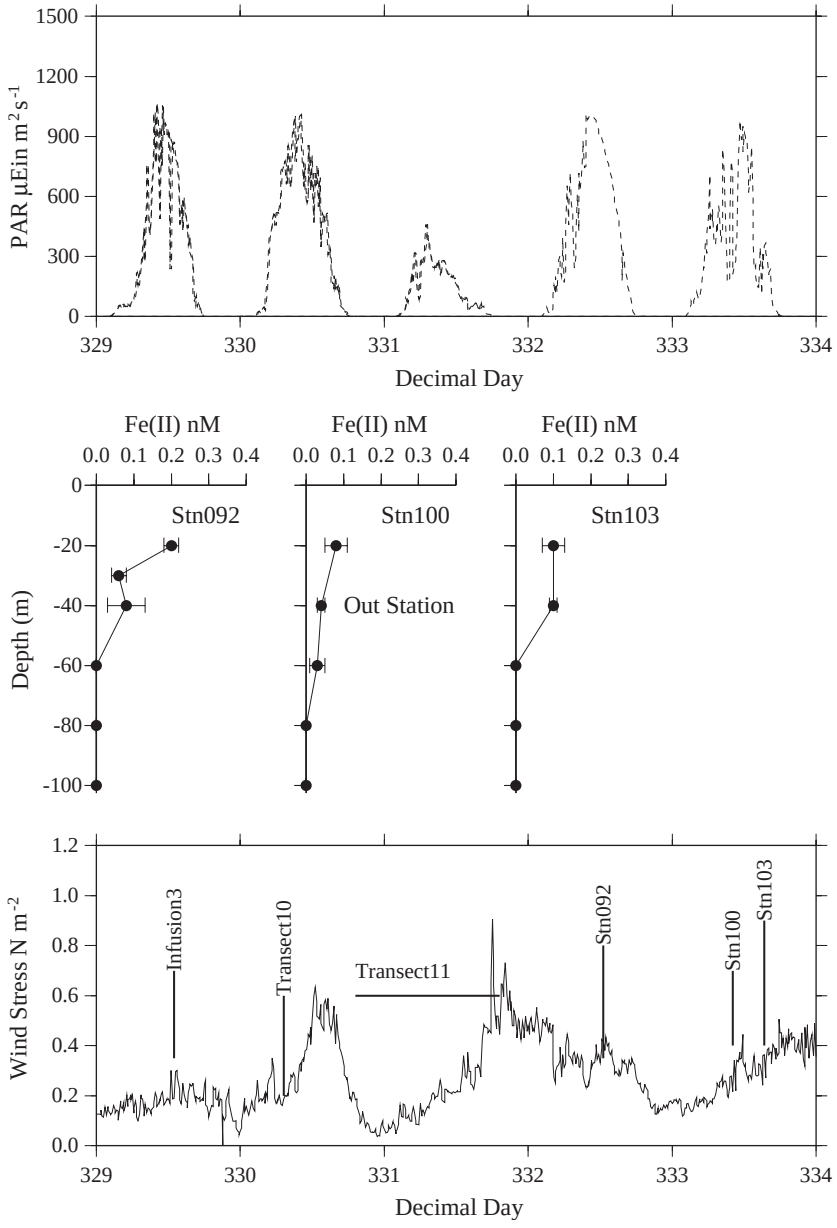

Fig. 4. Time course of vertical distribution of Fe(II) after the third iron infusion during EisenEx. Top: Photosynthetically available radiation (PAR: 400–700 nm). Centre: H_2O_2 and Fe(II) vertical distributions. Bottom: Wind stress and station timeline.

2001; Watson and Ledwell, 1990) and assuming Fickian diffusion.

$$\sigma^2 = 2K_z t$$

As the SF_6 was already well mixed throughout the mixed layer, it is not possible to use it as a tracer here. Using this approach, estimates of the vertical diffusivity constant, K_z, for the 2-day period between the occupation of Stations 46 and 49 could be obtained. There was good agreement between the values found for DFe, K_z=6.7±0.7 cm^2 s^{-1}, and TFe, K_z=6.0±0.6 cm^2 s^{-1}. Fe(II) itself gave a much

lower estimate, K_z=2.0±1.1 cm^2 s^{-1}, but it was also subject to oxidative losses during this time. The behavior of DFe and TFe at this time is very different to that encountered in previous iron enrichment experiments where iron has been rapidly lost from the mixed layer within a few hours(Bowie et al., 2001; Coale et al., 1998).

Dissolved and total iron is not normally a conservative tracer so how does this condition arise? During this period of observation, there was a minor storm with wind stress approaching 0.5 N m^{-2} and heavy cloud (Fig. 3). Significantly at this time there was heavy rain, estimated at 25 mm over the 2-day period (onboard rain gauge). This heavy rain apparently created a rain-formed mixed layer (Price, 1979) as can be clearly seen in the salinity and density profiles from this time (Fig. 5a,d), while there was only a slight warming (Fig. 5b) during this time. Dissolved iron (Fig. 5c) was apparently trapped between the rain-formed mixed layer and the early mixed layer; this may have accounted for its slow removal. Most of the iron at this time (Nishioka et al., 2004) was truly soluble (less then 200 kDa) or colloidal (between 200 kDa and 0.2 μm) and thus with a low Stokes settling velocity and would not be expected to sink out over 2 days. Consideration of the freshwater input from the

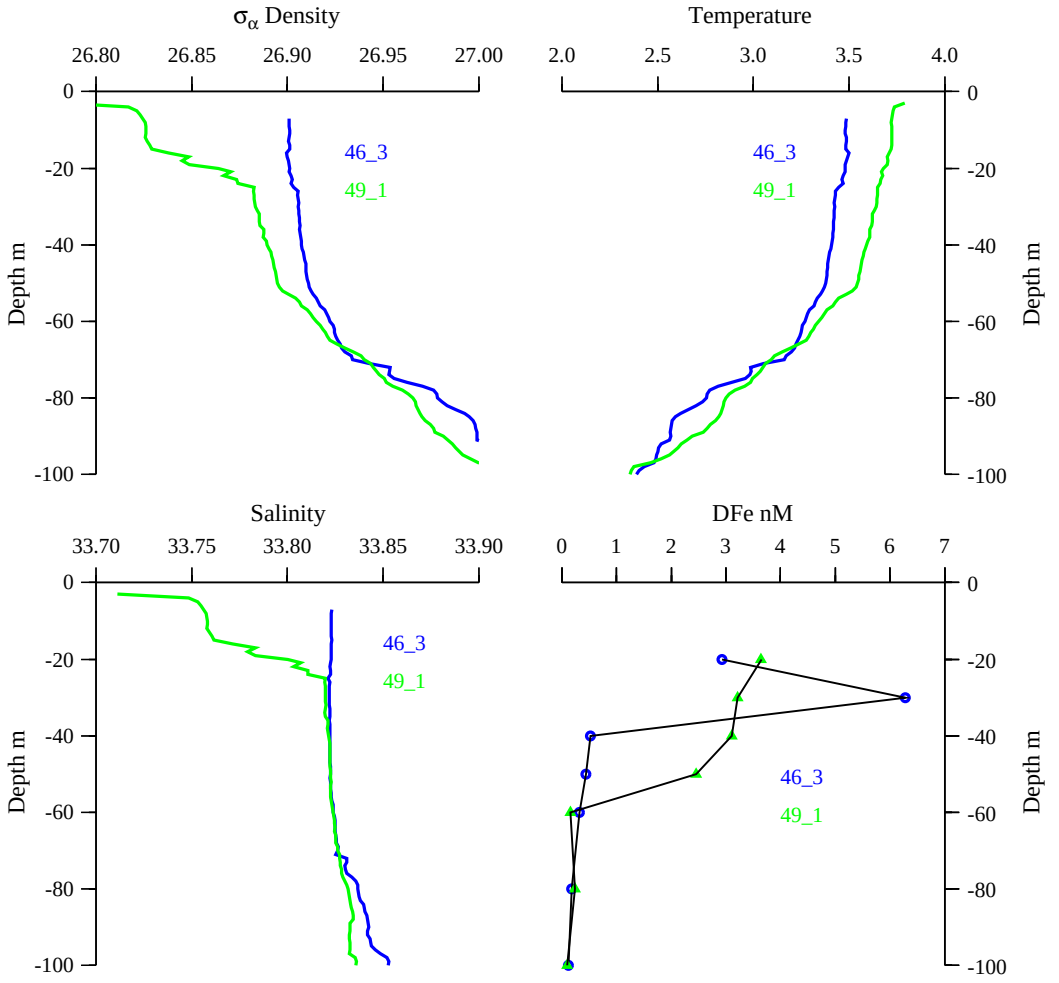

Fig. 5. Hydrographic parameters for Stations 46 and 49 in EisenEx. Clockwise from top left: (a) density, (b) temperature, (c) dissolved iron and (d) salinity.

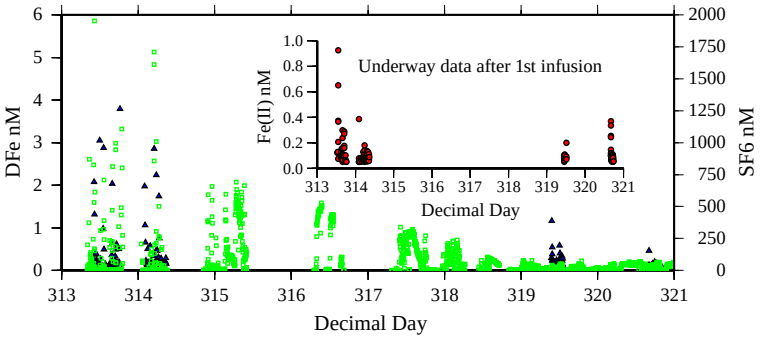

Fig. 6. Horizontal distributions of Fe(II) (circles, insert), DFe (triangles) and the SF_6 anomaly (squares) from surface transects during the period between the first and second iron infusions in EisenEx. SF_6 anomaly concentrations are derived from underway values, corrected for the out patch background SF_6 concentration (~2 fmol L^{-1}).

salinity depression is consistent with a 25-mm addition, also there were no icebergs present at this time so ice melt was not a factor.

There have been few other studies estimating K_z within the mixed layer, as opposed to across the pycnocline. McCarthy et al. (1992) used ^{15}N uptake rates to estimate K_z through the water column in a warm core ring in the Gulf Stream. They found values of 0.8–300 cm^2 s^{-1}, with the highest values after the passage of a storm system. Recent work on the Southern Ocean based on CTD and ADCP data (Garabato et al., 2004) suggests a range of K_z values from 0.1 to 1 cm^2 s^{-1} for the upper 300 m of the APF and SACC. Thus the values estimated here seem to be consistent with early work.

The slow mixing after the second infusion does not appear to have lasted more than 2 days, as by 4 days after the infusion, the rain-formed mixed layer was gone and Fe(II) and DFe concentrations had decreased markedly. A major storm system (Beaufort 9–10) then passed through the patch on DD325 and this also halted any shipboard operations so no further analysis was possible at this time.

3.6. Fe(II) horizontal distribution

Surface transects of Fe(II) were run in conjunction with the underway mapping of SF_6 and DFe throughout much of EisenEx (Table 1). Figs. 6 and 7 show a comparison of SF_6, DFe and Fe(II) as a function of time; note that each measurement operated on a different sampling frequency of ~3.5 min, 10 min and 90 s, respectively. Only Fe(II) values that are higher than the *limit of quantification* are shown; this

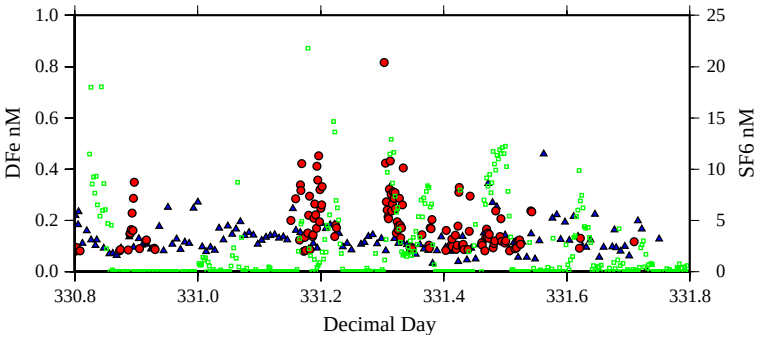

Fig. 7. Horizontal distributions of Fe(II) (circles, insert), DFe (triangles) and SF_6 anomaly (squares) from surface transects during the period of the large scale mapping (transect 11) in EisenEx. SF_6 anomaly concentrations are derived from underway values, corrected for the out patch background SF_6 concentration (~2 fmol L^{-1}). Note the presence of appreciable Fe(II) when there is no SF6 anomaly; this Fe(II) is believed to have been derived from rainwater as it was raining considerably during this transect.

limit varied between transect runs (50–120 pM) depending mostly on the age of the luminol reagent.

Overall, there was apparently good agreement between the presence of Fe(II) or DFe and SF_6 as would be expected, though a complete statistical analysis is not warranted for several reasons: (a) Initially after the first infusion, it is apparent that the SF_6 was detectable in surface waters at significant concentrations before any Fe signal had mixed up, presumably from transport by bubbles. (b) Subsequent infusions of iron, referred to as the 'patch within a patch', do not correlate at all to the overall patch marked by the SF_6 nor in many cases to the daily position of the SF_6 maximum.

Sharp gradients can be seen in Fe(II), DFe on several occasions, most notably in the days after an infusion. In this study and SOIREE (Croot et al., 2001), Fe(II) was still detectable several days after an iron infusion. In SOIREE, limited measurements for Fe(II) in surface waters was made and no vertical profiles were performed, but there Fe(II) was found to be an appreciable fraction of the surface DFe even up to 4 days after the last infusion (Croot et al., 2001) during a period of low wind mixing. In the present study, we found that during the initial part of the study when wind mixing was lowest, Fe(II) was still detectable 7 days after the initial infusion (Fig. 6).

Transect 11 (Fig. 7) was a 24-h full survey of the SF_6 patch near the end of the experiment when surface SF_6 concentrations were significantly diluted, due to the increase in patch volume, since the first infusion. During transect 11, elevated Fe(II) concentrations (200–300 pM) were detected several times in the absence of SF_6 (see Fig. 7). These events corresponded with a series of rain showers (unfortunately, the ship's rain gauge was now not functioning) and subsequently the opportunity was taken to obtain a rain sample using a trace metal clean funnel, while the ship was heading into the wind (to minimize contamination). Analysis on the rain collected (2.08 mm during DD 331.635–331.75) showed TFe=260±20 nM, which is higher than previously reported for rain passing over the Southern Ocean, in the vicinity of New Zealand, 16–47 nM (Arimoto et al., 1990; Halstead et al., 2000). Back trajectory calculations (NOAA air resources laboratory—data not shown) indicated that the air mass associated with the rain had originated from near the surface in southern Patagonia, 4 days earlier, and thus potentially contained appreciable iron rich dust (Gaiero et al., 2003). Estimates of the Fe(II) content by the same technique as for seawater were hampered by matrix problems, presumably from the high H_2O_2 concentrations in the rain and the presence of organic material and so only a lower bound of 40±20 nM was possible. Fe(II) has also previously been measured in rainwater samples from coastal regions (Kieber et al., 2001b,c; Willey et al., 2000) and is believed to be produced from photoreduction of aerosol iron. This single shower if diluted initially into the upper 2–10 m, the active mixed layer, would have contributed ~0.1–0.5 nM Fe(II), roughly consistent with the data in Fig. 7.

3.7. H_2O_2 vertical distribution

H_2O_2 data was collected only during the period of the cruise between infusions 2 and 3 (Table 1; Appendix A). As far as we are aware, H_2O_2 has not been measured during any previous iron enrichment experiment. Vertical profiles of H_2O_2 are shown in Fig. 3 and show a range of concentrations from below detection at depth to a maximum of 30 nM, consistent with other studies in the Southern Ocean (Resing et al., 1993; Sarthou et al., 1997; Weller and Schrems, 1993; Yocis et al., 2000).

Interestingly, the H_2O_2 profiles immediately after the second infusion show a distinct minimum at the same depth (30 m) as the maximum Fe(II) concentration (Station 46, Fig. 5). This minimum in H_2O_2 then expands and propagates over the next two days (Station 49, Fig. 5) to be present over the lower half of the mixed layer. This minima for H_2O_2 is consistent with removal by oxidation of Fe(II), showing the effects of the iron enrichment on a major oxidant of Fe(II). Other possible processes which remove H_2O_2, such as biological activity (Wong et al., 2003), would not be expected to show the same dispersion pattern. As discussed above, during this time, a rain mixed layer had formed in the upper 20 m and was preventing mixing below this level. The rainfall would have introduced H_2O_2 into the upper waters, as typically rain or snow samples contain μM concentrations. An estimate of the H_2O_2 injection from the rain during this time can be gathered from comparison with snow samples from King George

Island, South Shetland Islands (62°S), which contained 10–13.6 μmol L^{-1} H_2O_2 (Abele et al., 1999), consistent with earlier data from the same region (Weller and Schrems, 1993). We can then estimate that 25 mm of rain would introduce an injection of 250–340 μmol m^{-2} H_2O_2. This is approximately 18–50% of the upper water column inventory (0–100 m) estimated for the period between infusions 2 and 3 during EisenEx (range 690–1400 μmol m^{-2}), indicating that precipitation is a major source of H_2O_2 to surface waters during EisenEx. However, during the period between Stations 46 and 49, the induced rain mixed layer would have prevented the H_2O_2 from precipitation from mixing down to below 20 m, where the Fe(II) maxima was found. This would similarly apply to photochemically produced H_2O_2 during this time, though PAR fluxes were also low during this time (Fig. 3).

Later profiles of H_2O_2 from inside the patch show a distinctive maximum at around 40 m (Station 83); this time, however, the Fe(II) concentration has been reduced to below detection limits. Thus maximum is however roughly consistent with the position of the chlorophyll fluorescence maximum at the time (not shown), suggesting either (a) biological production by the biota (Palenik et al., 1987) or (b) more photochemical labile DOC (Dissolved Organic Carbon) from phytoplankton exudation. DOC concentrations measured during EisenEx show no systematic trends over the duration of the experiment (S. Gonzalez, personal communication), though concentrations are elevated in the mixed layer at Station 83 (range 70–90 μmol L^{-1}) compared to other stations (range 50–70 μmol L^{-1}). However, we have no information on the photo lability of this extra DOC and when coupled with the low light flux at 40 m it is more likely that some biological process is responsible for the deep H_2O_2 source at this time. Palenik et al. (1987) showed that while the diatom *Thalassiosira weissflogii* did not produce H_2O_2, the Prymnesiophyte *Hymenomonas carterae* did from cell-surface redox enzymes that did not seemingly involve an O_2^- intermediate. They suggested that this redox enzyme may be involved in direct nutrient transport, antibacterial activity or in redox activity necessary to acquire trace nutrients (reduction of iron) or nitrogen (oxidation). More recently, it has been shown in some algal cultures that H_2O_2 production increases under conditions of iron limitation, possibly through enhanced ferric chelate reductase activity (Middlemiss et al., 2001; Twiner and Trick, 2000; Weger et al., 2002). Dissolved iron concentrations at Station 83 were very low throughout the mixed layer (40–90 pM) and almost back to pre-infusion ambient levels, thus this mechanism of H_2O_2 production seems plausible. This topic requires further investigation to examine these processes in more detail and to examine the physiological mechanisms that produce H_2O_2.

3.8. Fe(II) oxidation rates

The oxidation rate of Fe(II) in samples at in situ temperatures was measured on a few occasions during the course of EisenEx (Croot and Laan, 2002). Typically half-lives for the oxidation were around 90 min, consistent with extrapolation of the laboratory data of Millero and Sotolongo (1989) and Millero et al. (1987) at the measured temperature and H_2O_2 concentration. Previous work in Southern Ocean waters has also found good agreement to extrapolations of the Millero values when H_2O_2 values are known (Croot, unpublished). During the infusion, H_2O_2 appears to be rapidly consumed by the added Fe(II) and is reformed by reactions between O_2, and subsequently O_2^-, and Fe(II). Steady-state concentrations of H_2O_2 should be reached relatively quickly.

The lowest temperatures at which laboratory Fe(II) oxidation experiments have been reported in the literature is at 5 °C (Kuma et al., 1992, 1995; Millero and Sotolongo, 1989; Millero et al., 1987) with most experimental data having been obtained at 25 °C. Similarly King and coworkers have shown the importance of carbonate speciation on the oxidation of Fe(II) by O_2 (King, 1998) and by H_2O_2 (King and Farlow, 2000). In the present case, we could find no data for the speciation of Fe(II) carbonate complexes at low temperatures and thus more laboratory work is required to extend these key parameters to temperatures typically encountered in Polar oceans and in the deep sea. Additionally, many laboratory studies on Fe(II) speciation and reactivity are performed at low pH in order to take advantage of the longer half-life, but in turn make application of the data to seawater pH difficult. Working at lower temperatures could achieve the same methodological aim and provide

more data which is directly applicable to polar oceans and deep waters.

4. Model results

To examine the role of O_2^- in maintaining Fe(II) in the water column, we applied a simple 1D chemical mixing model to the initial conditions found immediately after the second infusion (see above). Values for the vertical diffusion coefficient K_z were fixed at 6 $cm^2\ s^{-1}$ for in the mixed layer (as determined above) and 0.3 $cm^2\ s^{-1}$ below (estimate from SF_6 mixing data). Temperature, pH and salinity where assumed constant, O_2 was assumed to be at 100% saturation throughout and H_2O_2 was set at 20 nM in the mixed layer and 0 below. Rate constants where taken from the literature (see Table 2) at the model temperature where possible. Presently we could find no literature data on the rates of reactions of O_2^- with Fe(II) or Fe(III) at temperatures other than 25 °C. For the present case, we used the 25 °C value when no other value was available. As the effect of temperature on the oxidation rates of Fe(II) for O_2 and H_2O_2 are caused largely by the enthalpy change for K_w (Millero and Sotolongo, 1989; Millero et al., 1987), it may be possible to correct the O_2^- similarly, but this has not been pursued here.

Fig. 8 shows the results of the two model runs. In the case with no O_2^-, the Fe(II) is oxidized with an hour and there is only a small loss of H_2O_2 at the depth of the iron infusion. The situation is very different when O_2^- is included as Fe(II) persists over the course of a day and is subsequently mixed through more of the mixed layer. Similarly the drawdown of H_2O_2 is amplified and expanded. The O_2^- case should be viewed as a maximal effect as it has been shown to undergo other reactions with Cu, DOM and other unknown pathways (Goldstone and Voelker, 2000; Petasne and Zika, 1987; Zafiriou et al., 1998) which would greatly reduce its effectiveness. Similarly, complexation of Fe(III) by organic ligands may hinder or stop altogether reaction 5 (Voelker and Sedlak, 1995).

The slow mixing seen after the second infusion allows a situation to develop where large concentrations of Fe(II) (this work) and truly dissolved Fe(III) (Nishioka et al., 2004) exist at levels well above that which could be supported by organic complexation. Indeed, during this time, high concentrations of colloidal Fe(III) was measured (Nishioka et al., 2004) and speciation measurements suggested only 50–80% of the dissolved iron was organically complexed (Boye et al., submitted for publication). Thus it does seem plausible that during this time, the presence of significant concentrations of dissolved or colloidal iron which could react with O_2^- to form Fe(II) was a major pathway for maintaining Fe(II) in solution (Fig. 9). Sunlight, and in particular UV radiation (Rijkenberg et al., in press), may however be a more important mechanism under normal low iron conditions in the open ocean (Croot et al., 2001).

4.1. Implications for iron redox speciation in seawater

At the low temperatures found in high latitude waters and in the deep sea, it now appears that three key factors may influence iron redox speciation: (1) Significantly longer half-lives for Fe(II) (Croot et al., 2001) compared to tropical waters. (2) Increased solubility of inorganic Fe(III) species (Liu and Millero, 2002). (3) The role of colloidal iron in regulating iron concentrations (Nishioka et al., 2001). Organic complexation obviously plays a major role in each of the factors outlined above by controlling the distribution and reactivity of the dissolved redox species. It remains then for future work to focus on the connectivity between organic complexation and the three factors mentioned above.

One key question arises from the present work—How important is the reaction between O_2^- and Fe(III) and is its importance in an iron enrichment experiment an anomalous occurrence? The data presented here do suggest that reaction (5) is occurring, as the alternative explanation of organic complexation retarding Fe(II) oxidation does not hold for the period immediately after the infusions as measurements at the time showed only a 90-min half-life. This is not to say that Fe(II) complexation by organic ligands does not occur merely that during an infusion, Fe(II) would presumably be present mostly as the free ion or as carbonate complexes as any organic complexing agents would be titrated out rapidly. An iron enrichment experiment is not an

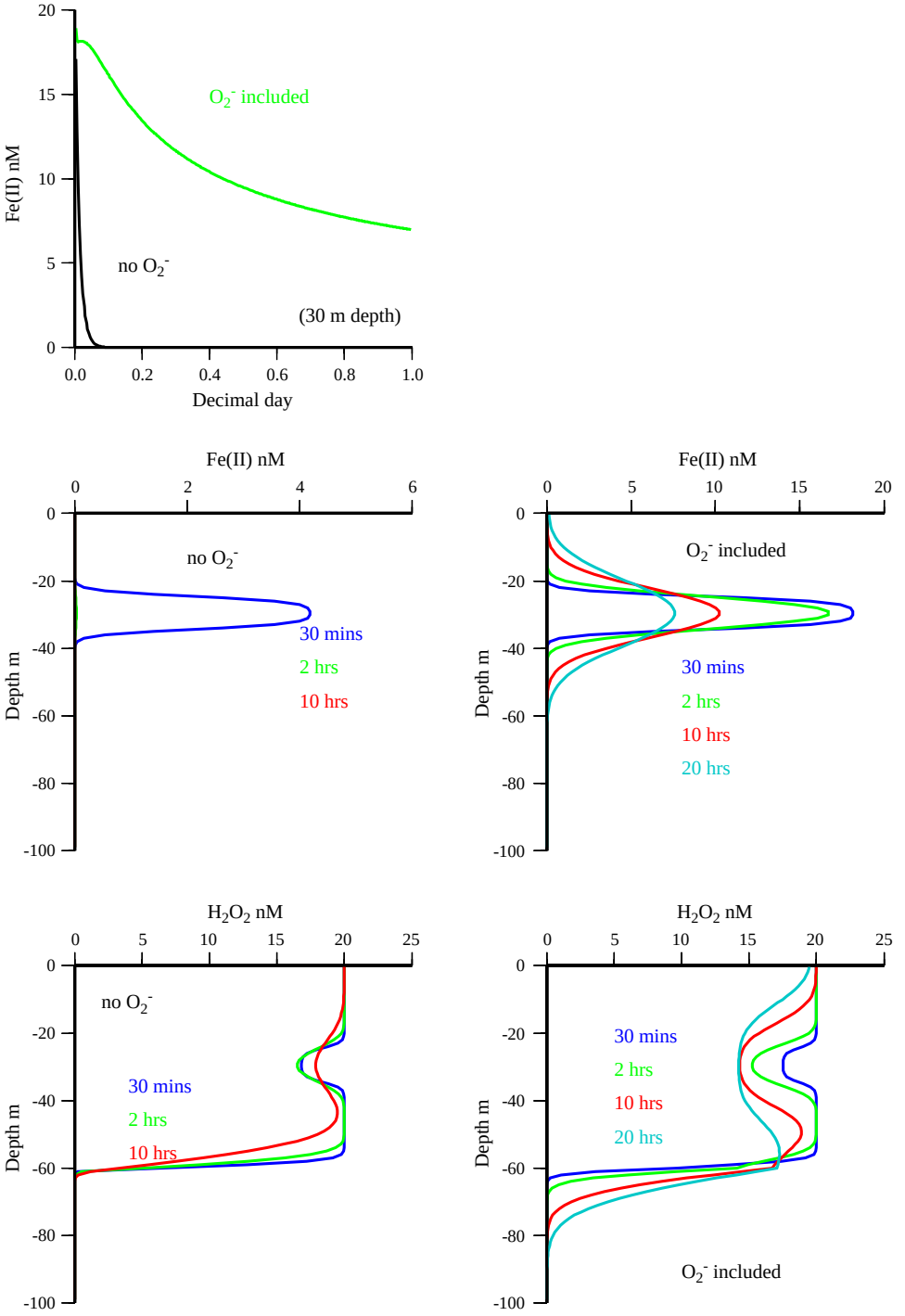

Fig. 8. Model results from finite difference 1D model showing the effects of O_2^- on the distribution of Fe(II) and H_2O_2. Note that in the case where there is no O_2^- included in the model, Fe(II) concentrations fall below 100 pmol L^{-1} within 2 h. See the text for more details.

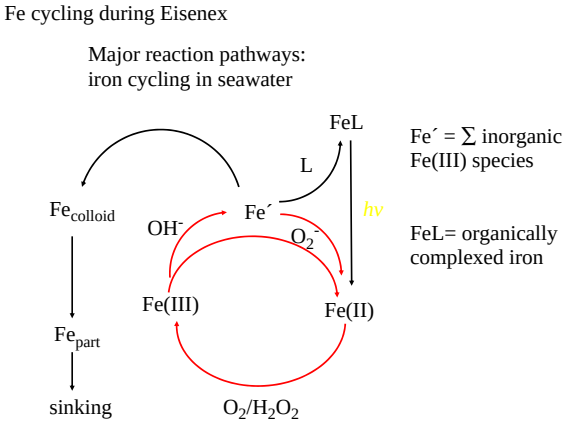

Fig. 9. Schematic showing the key processes affecting the redox cycling of iron during EisenEx.

ordinary process in the Southern Ocean, despite it occurring frequently in the last few years, and thus the situation reported here must be viewed as an experimentally derived artifact. However, reaction (5) could also be significant in the natural system under the right conditions—this however remains to be tested in the open ocean, non-iron enrichment conditions.

4.2. Implications for iron measurements

The data collected here on several occasions show significant differences between DFe, as measured by the luminol H_2O_2 chemiluminescence method (de Jong et al., 1998; Obata et al., 1993, 1997), and Fe(II) as measured by luminol chemiluminescence (Croot and Laan, 2002). The main reason for this discrepancy appeared to be the long half-life of the Fe(II) and the loading pH employed with the Fe(III) method. Work by de Jong et al. (1998) showed that Fe(II) was only loaded onto the preconcentration columns used in the present study at a pH>5, thus at the loading pH of 4.5 used in this study, Fe(II) would be poorly recovered. In all cases during EisenEx seawater samples were acidified and left at room temperature for at least 1 h before analysis. However, immediate acidification could stabilize the Fe(II) and thus lead to a potential underestimation of DFe. We recommend future work should allow the Fe(II) to oxidize before acidification. An alternative method suggested by Ken Johnson (MBARI) is to add H_2O_2 to the acidified samples to oxidize the Fe(II). Work during EisenEx also found that the presence of strong iron binding ligands can also lead to an underestimation of the DFe concentration (Croot et al., submitted for publication).

5. Conclusion

Measurements of Fe(II) and H_2O_2 made during an iron enrichment experiment in the Southern Ocean, EisenEx, show strong interactions between the two chemical species. The addition of Fe(II) to the seawater saw a reduction of H_2O_2 in the iron plume as the Fe(II) was oxidized by H_2O_2 and O_2. Vertical profiles of Fe(II) and surface transects showed that the Fe(II) existed for up to 8 days after an infusion, through most likely a combination of organic complexation retarding oxidation and formation through reduction of Fe(III) by O_2^-. The reaction between Fe(III) and O_2^-, generated photochemically or more likely here from the reduction of O_2 during reaction with Fe(II), appeared to be a major pathway for formation of Fe(II) in this experiment.

Acknowledgments

We especially thank the assistance and logistical support provided by the officers and crew of the *P.S. Polarstern*, in particular the deck crew for their unflagging enthusiasm for deploying the towed fish in all weathers. Thanks also to the Chief Scientist Victor Smetacek, Uli Bathmann for all their efforts during EisenEx. Financial support for P.L.C was provided by NEBROC (Netherlands Bremen Oceanography). Thanks to M Rijkenberg and L Gerringa for setting up the H_2O_2 system used during this study. Bob Leben, Univeristy of Colorado, Boulder is gratefully acknowledged for his help with the SSH-anomaly data. This manuscript was greatly improved by comments from Whitney King, Cliff Law and Joan D. Willey. This work was also partly financed by the European Community projects IRONAGES (EVK2-CT1999-00031) and CARUSO (ENV4-CT97-0472).

Appendix A

Fe(II), dissolved iron (DFe) and H_2O_2 measurements from vertical casts during the EisenEx experiment

Station	Latitude	Longitude	Date (time)	Depth (m)	[Fe(II)], nmol L^{-1}	[DFe], nmol L^{-1}	H_2O_2, nmol L^{-1}
046	48°20.30′S	21°01.10′E	16.11	20	0.60±0.05	2.92	21.4
DD321			(14:00)	30	1.00±0.07	6.28	7.1
IN				40	0.06±0.01	0.52	22.2
				50	0.05±0.04	0.44	20.6
				60	0.10±0.06	0.32	5.5
				80	b.d.	0.18	b.d.
				100	b.d.	0.12	–
049	48°20.70′S	20°53.29′E	18.11	20	0.17±0.05	3.65	22.7
DD323			(12:30)	30	0.25±0.02	3.22	9.0
IN				40	0.22±0.02	3.11	10.4
				50	0.19±0.04	2.45	10.0
				60	0.03±0.01	0.15	14.7
				80	b.d.	0.24	9.7
054	48°21.00′S	20°38.12′E	19.11	20	b.d.	0.07	25.3
DD324			(15:15)	30	b.d.	0.10	26.3
OUT				40	b.d.	0.10	28.4
				60	b.d.	0.15	33.7
				80	b.d.	0.05	20.0
055	48°18.70′S	20°40.16′E	19.11	20	b.d.	0.04	25.5
DD324			(17:20)	30	b.d.	0.04	21.1
OUT				40	b.d.	0.03	26.9
				60	b.d.	0.02	12.4
				80	b.d.	0.10	4.4
061	48°10.40′S	20°42.45′E	20.11	20	0.19±0.02	0.93	12.2
DD325			(00:10)	30	0.03±0.04	3.15	13.0
IN				40	0.12±0.07	1.37	17.0
				50	b.d.	0.70	15.7
				60	b.d.	0.06	18.3
				80	b.d.	0.03	12.2
				100	b.d.	0.02	6.7
081	48°00.68′S	21°00.64′E	23.11	20	b.d.	0.09	23.5
DD328			(11:00)	30	b.d.	0.20	25.2
IN				40	b.d.	0.12	13
				60	b.d.	0.11	10.4
				80	b.d.	0.07	5.2
083	48°07.43′S	21°01.06′E	23.11	20	b.d.	0.09	18.0
DD328			(15:10)	30	b.d.	0.07	25.1
IN				40	b.d.	0.04	29.8
				60	b.d.	0.05	22.0
				80	b.d.	0.06	7.8
086	48°02.23′S	21°06.46′E	23.11	20	b.d.	0.04	23.5
DD328			(21:30)	30	b.d.	0.08	22.7
IN				40	b.d.	0.09	14.1
				60	b.d.	0.08	11.8
				80	b.d.	0.03	11.0
092	48°07.44′S	21°08.48′E	27.11	20	0.20±0.02	0.19	–
DD332			(12:30)	40	0.06±0.02	0.19	–
IN				60	0.08±0.05	0.14	–
				80	b.d.	0.21	–
				100	b.d.	0.12	–
100	48°08.80′S	21°00.01′E	28.11	20	0.08±0.03	0.12	–

Appendix A (*continued*)

Station	Latitude	Longitude	Date (time)	Depth (m)	[Fe(II)], nmol L^{-1}	[DFe], nmol L^{-1}	H_2O_2, nmol L^{-1}
DD333			(10:00)	40	0.04±0.01	0.10	–
OUT				60	0.03±0.02	0.09	–
				80	b.d.	0.15	–
				100	b.d.	0.12	–
103	48°00.00′S	21°00.19′E	28.11	20	0.10±0.03	0.67	–
DD333			(15:15)	40	0.10±0.01	0.60	–
IN				60	b.d.	0.70	–
				80	b.d.	0.25	–
				100	b.d.	0.15	–

b.d. denotes below detection limit of technique. DD is decimal day, using the convention that midday on the 1.1.2000 is Julian day 1.5. All times are UTC.
Station 106: all samples b.d.

References

Abele, D., Ferreyra, G.A., Schloss, I., 1999. H_2O_2 accumulation from photochemical production and atmospheric wet deposition in Antarctic coastal and off-shore waters of Potter Cove, King George Island, South Shetland Islands. Antarctic Science 11 (2), 131–139.

Abraham, E.R., et al., 2000. Importance of stirring in the development of an iron-fertilised phytoplankton bloom. Nature 407, 727–730.

Arimoto, R., et al., 1990. Concentrations, sources and fluxes of trace elements in the remote marine atmosphere of New Zealand. Journal of Geophysical Research 95, 22389–22405.

Bellerby, R., Olsen, A., Johannessen, T., Croot, P., 2002. The Automated Marine pH sensor (AMpS); a high precision continuous spectrophotometric method for seawater pH measurements. Talanta 56, 61–69.

Bowie, A.R., et al., 2001. The fate of added iron during a mesoscale fertilisation experiment in the Southern Ocean. Deep-Sea Research. Part 2. Topical Studies in Oceanography 48, 2703–2743.

Boyd, P.W., Law, C.S., 2001. The Southern Ocean Iron RElease Experiment (SOIREE)—introduction and summary. Deep-Sea Research. Part 2. Topical Studies in Oceanography 48, 2425–2438.

Boye, M., et al., 2001. Organic complexation of iron in the Southern Ocean. Deep Sea Research 48, 1477–1497.

Boye, M., et al., 2004. Temporal variations in iron organic complexation during an open ocean mescoscale iron enrichment in the Southern Ocean (EisenEx). Marine Chemistry (submitted for publication).

Byrne, R.H., Kump, L.R., Cantrell, K.J., 1988. The influence of temperature and pH on trace metal speciation in seawater. Marine Chemistry 25, 163–181.

Coale, K.H., et al., 1996. A massive phytoplankton bloom induced by an ecosystem-scale iron fertilization experiment in the equatorial Pacific Ocean. Nature 383, 495–501.

Coale, K.H., et al., 1998. IronEx-I, an insitu iron-enrichment experiment: experimental design, implementation and results. Deep-Sea Research. Part 2. Topical Studies in Oceanography 45, 919–945.

Cooper, W.J., Zika, R.G., Petasne, R.G., Plane, J.M.C., 1988. Photochemical formation of H_2O_2 in natural waters exposed to sunlight. Environmental Science and Technology 22, 1156–1160.

Croot, P.L., Hunter, K.A., 2000. Determination of Fe(II) and total iron in natural waters with 3-(2-pyridyl)-5,6-diphenyl-1,2,4-triazine (PDT). Analytica Chimica Acta 406, 289–302.

Croot, P.L., Johansson, M., 2000. Determination of iron speciation by cathodic stripping voltammetry in seawater using the competing ligand 2-(2-Thiazolylazo)-*p*-cresol (TAC). Electroanalysis 12 (8), 565–576.

Croot, P.L., Laan, P., 2002. Continuous shipboard determination of Fe(II) in Polar waters using flow injection analysis with chemiluminescence detection. Analytica Chimica Acta 466, 261–273.

Croot, P.L., et al., 2001. Retention of dissolved iron and Fe^{II} in an iron induced Southern Ocean phytoplankton bloom. Geophysical Research Letters 28, 3425–3428.

Croot, P.L., et al., 2004. Where does all the iron go? The fate of the added iron during the EISENEX iron enrichment experiment. Marine Chemistry (submitted for publication).

Csanady, G.T., 1978. An analysis of dumpsite diffusion experiments. In: Park, P.K. (Ed.), Ocean Dumping of Industrial Wastes. Plenum Press, New York, pp. 109–129.

de Baar, H.J.W., Boyd, P.W., 1999. The role of iron in plankton ecology and carbon dioxide transfer of the global oceans. In: Hanson, R.B., Ducklow, H.W., Field, J.G. (Eds.), The Dynamic Ocean Carbon Cycle: A Midterm Synthesis of the Joint Global Ocean Flux Study. International Geosphere Biosphere Programme Book Series. Cambridge University Press, pp. 61–140.

de Jong, J.T.M., et al., 1998. Dissolved iron at subnanomolar levels in the Southern Ocean as determined by ship-board analysis. Analytica Chimica Acta 377, 113–124.

Dentler, F.-U., 2001. Meteorologische Bedingungen. Berichte zur Polar- und Meeresforschung 400, 67–72.

DOE, 1994. Handbook of Methods for the Analysis of the Various Parameters of the Carbon Dioxide System in Sea Water. Ver. 2. ORNL/CDIAC-74. Oak Ridge National Laboratory.

Dunford, H.B., 2002. Oxidations of iron(II)/(III) by hydrogen peroxide: from aquo to enzyme. Coordination Chemistry Reviews 233/4, 311–318.

Emmenegger, L., King, D.W., Sigg, L., Sulzberger, B., 1998. Oxidation kinetics of Fe(II) in a eutrophic Swiss Lake. Environmental Science and Technology 32, 2990–2996.

Gaiero, D.M., Probst, J.-L., Depetris, P.J., Bidart, S.M., Leleyter, L., 2003. Iron and other transition metals in Patagonian riverborne and windborne materials: geochemical control and transport to the southern South Atlantic Ocean. Geochimica et Cosmochimica Acta 67, 3603–3623.

Garabato, A.C.N., Polzin, K.L., King, B.A., Heywood, K.J., Visbeck, M., 2004. Widespread intense turbulent mixing in the Southern Ocean. Science 303 (5655), 210–213.

Gervais, F., Riebesell, U., Gorbunov, M.Y., 2002. Changes in primary productivity and chlorophyll *a* in response to iron fertilization in the Southern Polar Frontal Zone. Limnology and Oceanography 47, 1324–1335.

Goldstone, J.V., Voelker, B.M., 2000. Chemistry of superoxide radical in seawater: CDOM associated sink of superoxide in coastal waters. Environmental Science and Technology 34, 1043–1048.

Gordon, R.M., Johnson, K.S., Coale, K.H., 1998. The behaviour of iron and other trace elements during the IronEx-I and PlumEx experiments in the Equatorial Pacific. Deep-Sea Research. Part 2. Topical Studies in Oceanography 45, 995–1041.

Halstead, M.J.R., Cunninghame, R.G., Hunter, K.A., 2000. Wet deposition of trace metals to a remote site in Fiordland, New Zealand. Atmospheric Environment 34, 665–676.

Johnson, K.S., Gordon, R.M., Coale, K.H., 1997. What controls dissolved iron concentrations in the world ocean? Marine Chemistry 57, 137–161.

Kieber, R.J., Cooper, W.J., Willey, J.D., Avery, G.B., 2001. Hydrogen peroxide at the Bermuda Atlantic Time Series Station: Part 1. Temporal variability of atmospheric hydrogen peroxide and its influence on seawater concentrations. Journal of Atmospheric Chemistry 39, 1–13.

Kieber, R.J., Williams, K., Willey, J.D., Skrabal, S., Avery, G.B., 2001. Iron speciation in coastal rainwater: concentration and deposition to seawater. Marine Chemistry 73, 83–95.

Kieber, R.K., Peake, B., Willey, J.D., Jacobs, B., 2001. Iron speciation and hydrogen peroxide concentrations in New Zealand rainwater. Atmospheric Environment 35, 6041–6048.

King, D.W., 1998. Role of carbonate speciation on the oxidation rate of Fe(II) in aquatic systems. Environmental Science and Technology 32, 2997–3003.

King, D.W., Farlow, R., 2000. Role of carbonate speciation on the oxidation of Fe(II) by H_2O_2. Marine Chemistry 70, 201–209.

King, D.W., Lounsbury, H.A., Millero, F.J., 1995. Rates and mechanism of Fe(II) oxidation at nanomolar total iron concentrations. Environmental Science and Technology 29, 818–824.

Kremer, M.L., 1999. Mechanism of the Fenton reaction. Evidence for a new intermediate. Physical Chemistry Chemical Physics 1 (15), 3595–3605.

Kuma, K., Nakabayashi, S., Suzuki, Y., Kudo, I., Matsunaga, K., 1992. Photo-reduction of Fe(III) by dissolved organic substances and existence of Fe(II) in seawater during spring blooms. Marine Chemistry 37, 15–27.

Kuma, K., Nakabayashi, S., Matsunaga, K., 1995. Photoreduction of Fe(III) by hydroxycarboxylic acids in seawater. Water Research 29, 1559–1569.

Kuma, K., Nishioka, J., Matsunaga, K., 1996. Controls on iron(III) hydroxide solubility in seawater: the influence of pH and natural organic chelators. Limnology and Oceanography 41, 396–407.

Large, W.G., Pond, S., 1981. Open ocean momentum flux measurements in moderate to strong winds. Journal of Physical Oceanography 11, 324–336.

Law, C.S., Watson, A.J., Liddicoat, M.I., 1994. Automated vacuum analysis of sulphur hexafluoride in seawater; derivation of the atmospheric trend 1970–1993 and potential as a transient tracer. Marine Chemistry 48, 57–69.

Law, C.S., Watson, A.J., Liddicoat, M.I., Stanton, T., 1998. Sulphur hexafluoride as a tracer of biogeochemical and physical processes in an open-ocean iron fertilisation experiment. Deep-Sea Research. Part 2. Topical Studies in Oceanography 45, 977–994.

Law, C.S., et al., 2001. A Langragian SF6 tracer study of an anticyclonic eddy in the North Atlantic: patch evolution, vertical mixing and nutrient supply to the mixed layer. Deep-Sea Research. Part 2. Topical Studies in Oceanography 48 (4–5), 705–724.

Lehninger, A.L., 1979. Biochemistry. Worth, New York. 1104 pp.

Liu, X., Millero, F.J., 2002. The solubility of iron in seawater. Marine Chemistry 77, 43–54.

Martin, J.H., Gordon, R.M., Fitzwater, S.E., Broenkow, W.W., 1989. VERTEX: phytoplankton/iron studies in the Gulf of Alaska. Deep-Sea Research 36, 649–680.

Martin, J.H., Fitzwater, S.E., Gordon, R.M., 1990. Iron deficiency limits phytoplankton growth in Antarctic waters. Global Biogeochemical Cycles 4, 5–12.

Martin, J.H., et al., 1994. Testing the iron hypothesis in ecosystems of the equatorial Pacific Ocean. Nature 371, 123–129.

Matthews, R.W., 1983. The radiation chemistry of aqueous ferrous sulfate solutions at natural pH. Australian Journal of Chemistry 36, 1305–1317.

McCarthy, J.J., Garside, C., Nevins, J.L., 1992. Nitrate supply and phytoplankton uptake kinetics in the euphotic layer of a Gulf-Stream Warm-Core Ring. Deep-Sea Research. Part A, Oceanographic Research Papers 39 (1A), S393–S403.

Middlemiss, J.K., Anderson, A.M., Stratilo, C.W., Weger, H.G., 2001. Oxygen consumption associated with ferric reductase activity and iron uptake by iron-limited cells of *Chlorella kessleri* (Chlorophyceae). Journal of Phycology 37 (3), 393–399.

Miller, W.L., Kester, D.R., 1988. Hydrogen-peroxide measurement in seawater by (*para*-hydroxyphenyl)acetic acid dimerization. Analytical Chemistry 60 (24), 2711–2715.

Millero, F.J., Sotolongo, S., 1989. The oxidation of Fe(II) with H_2O_2 in seawater. Geochimica et Cosmochimica Acta 53, 1867–1873.

Millero, F.J., Sotolongo, S., Izaguirre, M., 1987. The oxidation kinetics of Fe(II) in seawater. Geochimica et Cosmochimica Acta 51, 793–801.

Millero, F.J., Yao, W., Aicher, J., 1995. The speciation of Fe(II) and Fe(III) in natural waters. Marine Chemistry 50, 21–39.

Mitchell, B.G., Brody, E.A., Holm-Hansen, O., McClain, C., Bishop, J., 1991. Light limitation of phytoplankton biomass and macronutrient utilization in the Southern Ocean. Limnology and Oceanography 36, 1662–1677.

Moffett, J.W., Zafiriou, O.C., 1990. An investigation of hydrogen peroxide in surface waters of Vineyard Sound with $H_2^{18}O_2$ and $^{18}O_2$. Limnology and Oceanography 35, 1221–1229.

Nishioka, J., Takeda, S., Wong, C.S., Johnson, W.K., 2001. Size-fractionated iron concentrations in the northeast Pacific Ocean: distribution of soluble and small colloidal iron. Marine Chemistry 74, 157–179.

Nishioka, J., et al., 2004. Change in the concentrations of iron in different size fractionations during an iron fertilization experiment in the Southern Ocean, EisenEx. Marine Chemistry 95, 51–63.

Obata, H., Karatani, H., Nakayama, E., 1993. Automated determination of iron in seawater by chelating resin concentration and chemiluminescence detection. Analytical Chemistry 65, 1524–1528.

Obata, H., Karatani, H., Matsui, M., Nakayama, E., 1997. Fundamental studies for chemical speciation of iron in seawater with an improved analytical method. Marine Chemistry 56, 97–106.

Okubo, A., 1971. Oceanic diffusion diagrams. Deep-Sea Research 18, 789–802.

Öztürk, M., Croot, P., Bertilsson, S., Abrahamsson, K., Karlson, B., David, R., Chierici, M., Sakshaug, E., 2004. Iron enrichment and photoreduction of iron under PAR and UV in the presence of hydrocarboxylic acid: Implications for phytoplankton growth in the Southern Ocean. Deep-Sea Research II 51 (22–24), 2841–2856.

Palenik, B., Morel, F.M.M., 1988. Dark production of H_2O_2 in the Sargasso Sea. Limnology and Oceanography 33, 1606–1611.

Palenik, B., Zafiriou, O.C., Morel, F.M.M., 1987. Hydrogen peroxide production by a marine phytoplankter. Limnology and Oceanography 32, 1365–1369.

Petasne, R.G., Zika, R.G., 1987. Fate of superoxide in coastal sea water. Nature 325, 516–518.

Petasne, R.G., Zika, R.G., 1997. Hydrogen peroxide lifetimes in south Florida coastal and offshore waters. Marine Chemistry 56 (3–4), 215–225.

Pierre, J.L., Fontecave, M., 1999. Iron and activated oxygen species in biology: the basic chemistry. BioMetals 12 (3), 195–199.

Plane, J.M.C., Zika, R.G., Zepp, R.C., Burns, L.A., 1987. Photochemical modeling applied to natural waters. In: Zika, R.G., Cooper, W.J. (Eds.), Photochemistry of Environmental Aquatic Systems, ACS Symposium Series. American Chemical Society, Washington, DC, pp. 215–224.

Price, J.F., 1979. Observations of a rain-formed mixed layer. Journal of Physical Oceanography 9, 643–649.

Price, J.F., Weller, R.A., Pinkel, R., 1986. Diurnal cycling: observations and models of the upper ocean response to diurnal heating, cooling, and wind mixing. Journal of Geophysical Research 91 (C7), 8411–8427.

Resing, J., Tien, G., Letelier, R., Karl, D.M., 1993. Palmer LTER: hydrogen peroxide in the Palmer LTER region: II. Water column distribution. Antarctic Journal of the United States 28, 227–229.

Rijkenberg, M.J.A., et al., 2004. The influence of UV irradiation on the photoreduction of iron in the Southern Ocean. Marine Chemistry (in press).

Rose, A.L., Waite, T.D., 2001. Chemiluminescence of luminol in the presence of iron(II) and oxygen: oxidation mechanism and implications for its analytical use. Analytical Chemistry 73, 5909–5920.

Rose, A.L., Waite, T.D., 2002. Kinetic model for Fe(II) oxidation in seawater in the absence and presence of natural organic matter. Environmental Science and Technology 36, 433–444.

Rue, E.L., Bruland, K.W., 1995. Complexation of Iron(III) by natural organic ligands in the central north pacific as determined by a new competitive ligand equilibration/adsorptive cathodic stripping voltammetric method. Marine Chemistry 50, 117–138.

Rush, J.D., Bielski, B.H.J., 1985. Pulse radiolytic studies of HO_2/O_2^- with Fe(II)/Fe(III) ions. The reactivity of HO_2/O_2^- with ferric ions, its implication on the occurrence of the Haber–Weiss reaction. Journal of Physical Chemistry 89, 5062–5066.

Santana-Casiano, J.M., Gonzalez-Davila, M., Rodriguez, M.J., Millero, F.J., 2000. The effect of organic compounds in the oxidation kinetics of Fe(II). Marine Chemistry 70, 211–222.

Sarthou, G., et al., 1997. Fe and H_2O_2 distributions in the upper water column in the Indian sector of the Southern Ocean. Earth and Planetary Science Letters 147, 83–92.

Scully, N.M., McQueen, D.J., Lean, D.R.S., Cooper, W.J., 1996. Hydrogen peroxide formation: the interaction of ultraviolet radiation and dissolved organic carbon in lake waters along a 43–75 degrees N gradient. Limnology and Oceanography 41 (3), 540–548.

Smetacek, V., 2001. EisenEx: international team conducts iron experiment in Southern Ocean. U.S. JGOFS News 11 (1), 11.

Stanton, T.P., Law, C.S., Watson, A.J., 1998. Physical evolution of the Iron-Ex-I open ocean tracer patch. Deep-Sea Research. Part 2. Topical Studies in Oceanography 45, 947–975.

Strass, V.H., et al., 2001. The physical setting of the Southern Ocean iron fertilisation experiment. Berichte zur Polar- und Meeresforschung 400, 94–130.

Theis, T.L., Singer, P.C., 1974. Complexation of iron(II) by organic matter and its effect on iron(II) oxygenation. Environmental Science and Technology 8, 569–573.

Tsuda, A., et al., 2003. A mesoscale iron enrichment in the western Subarctic Pacific induces a large centric diatom bloom. Science 300 (5621), 958–961.

Turner, D.R., Whitfield, M., Dickson, A.G., 1981. The equilibrium speciation of dissolved components in freshwater and seawater at 25C and 1 atm pressure. Geochimica et Cosmochimica Acta 45, 855–881.

Twiner, M.J., Trick, C.G., 2000. Possible physiological mechanisms for production of hydrogen peroxide by ichyotoxic flagellate *Heterosigma akashiwo*. Journal of Plankton Research 22, 1961–1975.

van den Berg, C.M.G., 1995. Evidence for organic complexation of iron in seawater. Marine Chemistry 50, 139–157.

Voelker, B.M., Sedlak, D.L., 1995. Iron reduction by photoproduced superoxide in seawater. Marine Chemistry 50, 93–102.

Voelker, B.M., Morel, F.M.M., Sulzberger, B., 1997. Iron redox cycling in surface waters: effects of humic substances and light. Environmental Science and Technology 31, 1004–1011.

Watson, A.J., Ledwell, J.R., 1990. Purposefully released tracers. In: Charnock, H., Lovelock, J.E., Liss, P.S., Whitfield, M. (Eds.), Tracers in the Ocean. Princeton University, Princeton, NJ, pp. 189–200.

Watson, A., et al., 2001. SF_6 measurements on EisenEx. Berichte zur Polar- und Meeresforschung 400, 76–79.

Weger, H.G., Middlemiss, J.K., Petterson, C.D., 2002. Ferric chelate reductase activity as affected by the iron-limited growth rate in four species of unicellular green algae (*Chlorophyta*). Journal of Phycology 38 (3), 513–519.

Weller, R., Schrems, O., 1993. H_2O_2 in the marine troposphere and seawater of the Atlantic ocean. Geophysical Research Letters 20, 125–128.

Willey, J.D., et al., 2000. Temporal variability of iron speciation in coastal rainwater. Journal of Atmospheric Chemistry 37, 185–205.

Wong, G.T.F., Dunstan, W.M., Kim, D.B., 2003. The decomposition of hydrogen peroxide by marine phytoplankton. Oceanologica Acta 26 (2), 191–198.

Xiao, C., Palmer, D.A., Wesolowski, D.J., Lovitz, S.B., King, D.W., 2002. Carbon dioxide effects on luminol and 1,10-phenanthroline chemiluminescence. Analytical Chemistry 74, 2210–2216.

Yocis, B.H., Kieber, D.J., Mopper, K., 2000. Photochemical production of hydrogen peroxide in Antarctic Waters. Deep-Sea Research. Part 1. Oceanographic Research Papers 47 (6), 1077–1099.

Yuan, J.C., Shiller, A.M., 2000. The variation of hydrogen peroxide in rainwater over the south and central Atlantic ocean. Atmospheric Environment 34 (23), 3973–3980.

Yuan, J., Shiller, A.M., 2001. The distribution of hydrogen peroxide in the southern and central Atlantic ocean. Deep-Sea Research. Part 2. Topical Studies in Oceanography 48, 2947–2970.

Zafiriou, O.C., Voelker, B.M., Sedlak, D.L., 1998. Chemistry of the superoxide radical (O-2(−)) in seawater: reactions with inorganic copper complexes. Journal of Physical Chemistry A 102 (28), 5693–5700.